Establish intelligent detection system to evaluate the sugar smoking of chicken thighs

Bo Wang,* Hongyao Yang,* Fenggui Lu,* Fangzhu Yu,* Xiaodan Wang,† Yufeng Zou,‡ Dengyong Liu,*,‡,[1] Jianbo Zhang,* and Wenyun Xia*

*College of Food Science and Technology, Bohai University, Jinzhou 121013, China; †College of Food Science and Engineering, Jilin University, Changchun 130062, China; and ‡Jiangsu Collaborative Innovation Center of Meat Production and Processing, Quality and Safety Control, Nanjing, 210095, China

ABSTRACT The objective of this study was to establish a standardized color detection method to achieve low-cost, rapid, nonintrusive and accurate characterization of the color change of smoked chicken thighs during the smoking process. This study was based on machine vision technology using the Mean algorithm, K-means algorithm and K-means algorithm + image noise reduction algorithm to establish 3 colorimetric cards for the color of sugar-smoked chicken thighs. The accuracy of the 3 colorimetric cards was verified by the K-medoids algorithm and sensory analysis, respectively. Results showed that all 3 colorimetric cards had significant color gradient changes. From the K-medoids algorithm, the accuracy of the colorimetric card produced by the Mean algorithm, K-means algorithm and K-means algorithm + image noise reduction algorithm was 87.2, 95.1, and 96.7%, respectively. Meanwhile, the verification results of the sensory analysis showed that the accuracy of the Mean algorithm, K-means algorithm and K-means algorithm + image noise reduction algorithm colorimetric card was 69.4, 80.9, and 79.2%, respectively. A comparative analysis found that the colorimetric cards produced by the K-means algorithm and K-means algorithm + image noise reduction have excellent accuracy. These 2 colorimetric cards could become a suitable method for rapid, low-cost, and accurate online color monitoring of smoked chicken.

Key words: colorimetric card, smoked chicken thighs, color, sugar-smoked, machine vision

2021 Poultry Science 100:101447
https://doi.org/10.1016/j.psj.2021.101447

INTRODUCTION

Smoking can enrich food with unique smoky aroma (Janky et al., 1975; Alakali et al., 2017), attractive smoky color (Siskos et al., 2005; Zhang et al., 2021a) and has been widely used in meat products, such as bacon, sausage, and smoked chicken (Sheldon et al., 1982; Schwert et al., 2011; Alakali et al., 2017). As one of the smoking methods, sugar smoking produces fewer and safer harmful substances and is a widely used way of smoking (Paravisini et al., 2015; Zhang et al., 2021a). Sugar-smoked chicken is a well-known traditional meat product in northern China for its attractive color and unique flavor (Zhang et al., 2020; Chang et al., 2021a). During the smoking process, when the furnace temperature is higher than 90°C, the Maillard reaction, caramelization reaction and lipid oxidation reaction will lead to brown skin color of the sugar-smoked chicken (Echavarría et al., 2012). Therefore, color attributes are an important indicator of process quality and a fundamental attribute of product acceptability, which are closely linked to the purchase decision of the consumer (Purlis, 2012; Chang et al., 2021b). The color attributes of smoked chicken can be evaluated by some conventional methods. For instance, spectrophotometric technique and chromatographic method can evaluate the pigment content indirectly. Color changes can also be measured directly by instrumental colorimetric analysis (Purlis, 2012) or by sensory analysis techniques (Chang et al., 2021b). Furthermore, methods for evaluating the color of smoked products, either by sensory analysis or by instrumental techniques are destructive, time-consuming, and noneconomical. Therefore, sensory analysis and instrumental techniques do not fit the conditions for routine online analysis in an industrial environment (Valous et al., 2009).

In this context, economic, objective and rapid color measurement have been pursued during the food smoking process. As a color analysis strategy technology, the computer vision system simulates the modes of capturing and interpreting information by the human eye and

Received June 12, 2020.
Accepted August 23, 2021.

[1]Corresponding author: jz_dyliu@126.com

allows objective measurement of color by correlating it with consumer acceptance characteristics or product parameters (Taheri-Garavand et al., 2019). The technique can significantly reduce the use of workers and material resources and effectively improve work efficiency. It has the advantages of excellent accuracy, rapid recognition, and nondestructiveness (Shi et al., 2018). Computer vision can be used to evaluate the color changes of the bread and cheese during processing and to classify the degree of browning during baking (Wang and Sun, 2003; Purlis and Salvadori, 2009). It results demonstrated that computer vision systems have potential applications in process control systems involving color changes in the food industry (Brosnan and Sun, 2004). However, it has great limitations due to the high temperatures of the furnace during smoking process and the differences in color obtained under different lights intensity (Taheri-Garavand et al., 2019).

On the other hand, the colorimetric card can be used for color selection, comparison and communication by reflecting the color on a material (paper) with a gradient change (Zhang et al., 2021b). Compared with computer vision technology, this card is a valuable, low-cost, rapid, and strong anti-interference tool to evaluate and report color change during the sugar smoking process (Misimi et al., 2007). Meanwhile, this method provides a uniform standard tool for a range of colors. Color detection can be achieved by simply putting the colorimetric card beside the sample, which can effectively solve color identification (Giuseppe et al., 2008; Reyescerecedo et al., 2018). So far, colorimetric cards are widely applied in daily life, such as biliary atresia (Roberta et al., 2020), coral health assessment (Bahr et al., 2020), GI bleeding assessment (Gary R et al., 1995), spinning fabric color detection (Zhang et al., 2021b), and formaldehyde levels (Vladimir et al., 2011). However, few articles combine machine vision technology with algorithms to develop colorimetric cards to identify the color of smoked meat products.

The images were preprocessed using the Deep Convolutional Generative Adversarial Networks (**DCGAN**) model of computer vision system. Three colorimetric cards were produced using the Mean algorithm, K-mean algorithm, and K-mean algorithm + image noise reduction algorithm. Then, a K-medoids algorithm was combined with a sensory analysis to verify the accuracy of the colorimetric cards. Finally, the colorimetric cards with the most robust ability to resist external interference, most straightforward operation and highest accuracy are chosen as suitable for the production management of the smoked chicken industry. This study establishes a corresponding foundation for the standardization of color evaluation in the smoked chicken industry.

MATERIAL AND METHODS

Sample Preparation

Chickens (*HY-LINE VARIETY BROWN*) were supplied by Liaoning Goubangzi Food Co., Ltd (Liaoning, China). All chickens have the same genetic background and have fed the same diet (complete formula feed). The age of the chickens was 450 ± 50 d (Mean ± SD). After 12 h of fasting, the hens were slaughtered, and only the chicken thighs were taken. Then, cool for 30 min, labeled and packaged. Finally, 272 chicken thighs were obtained with an average weight of 160 ± 10 g (Mean ± SD). The diameter of the chicken thighs was approximately 5.5 cm, without peeling. All samples were transferred to the laboratory of Bohai University under the controlled temperature using a cooling box (2−4°C).

The smoked chicken thighs were prepared by reference to the traditional Goubangzi sugar-smoking process. All the possible colors of the smoked chicken thighs during the sugar smoking process were obtained by controlling the smoking time. A total of 272 chicken thighs were prepared and blanched to remove the bubbles. The chicken thighs were boiled in the brine with the following additives (g/L water): salt (25 g), pepper (2.5 g), aniseed (2.5 g), ginger (2.5 g), garlic (1 g), clove (1 g), onion (1 g), cardamom (0.5 g), cinnamon (0.5 g), and wine (4.5 g) at 90 to 95°C for 10 min, followed by a simmer treatment for 90 min. The chicken thighs were removed from the brine and cooled to room temperature (25 ± 5°C). The 272 chicken thighs were divided into 17 groups of 16 thighs each.

When the temperature of the sugar heating plate in the sugar fuming furnace (YXDT1/1, Hebei Xiaojin Machinery Manufacturing Co., Ltd. Heibei, China) reached 330°C, 60 g of sucrose was added to start smoking. After the temperature of the furnace reached 100°C, set the smoking time to start sugar smoking. The first group was smoked for 0 min, and the second group was smoked for 1 min, and so on. Sucrose was discarded after each period and new sugar was added. After cooling at room temperature, the water and oil stains were removed from the surface of the smoked chicken thighs, and images of the smoked chicken thighs were collected.

Acquisition of Images

To avoid the influence of external conditions on the experimental results and minimize experimental errors, the white background illumination chamber of 50 × 50 × 50 cm (W × H × L) was constructed with a 15.2 w (6500 K) ring shadowless lamp (HPR200, LOTS, Guangdong, China). The camera (EOS-M5, Canon, Tokyo, Japan) was fixed vertically on the top of the illumination chamber (Figure 1).

The collection process was as follows: The device was placed on a horizontal working platform. Adjust the distance between the camera lens and the sample surface. Open the device and collect images transmitted to the computer through the image acquisition card (VGA2 USB, Epiphan, Ottawa,ON, Canada). The image processing program written on the Python platform was used to analyze the data. The smoked chicken thighs were flipped horizontally by 90°, and 4 images were collected for each smoked chicken thigh. The images were

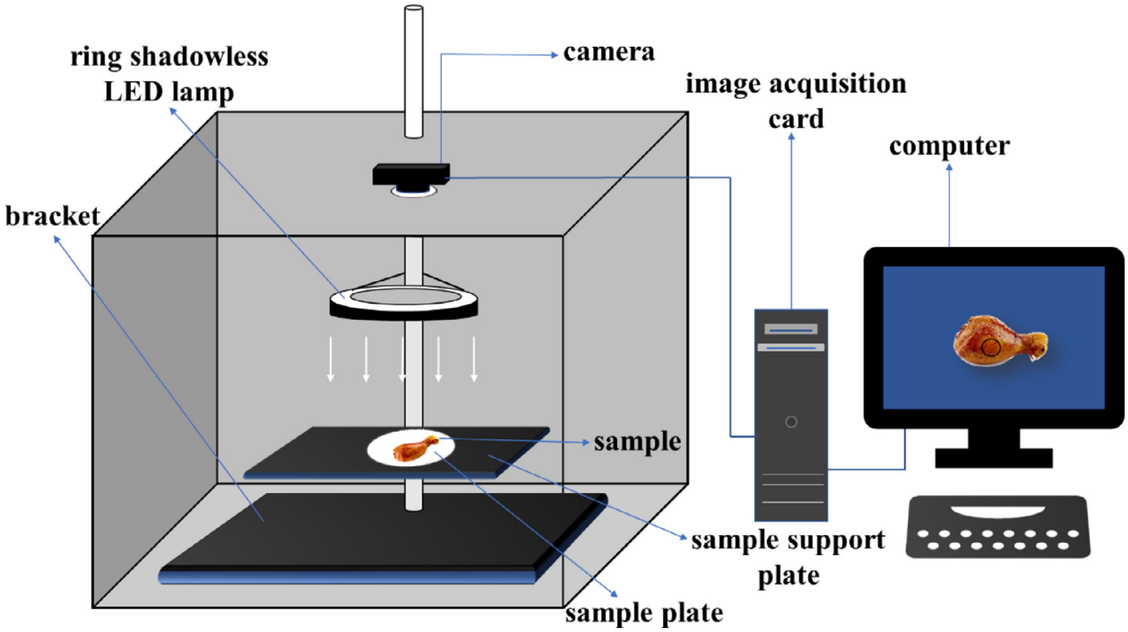

Figure 1. Computer vision acquisition system.

represented in RGB color space and had a resolution of 2,448 × 2,048 pixels in PNG format.

Color Measurement

The surface color of the skin-covered chicken thighs was determined using a colorimeter (CR-400, Konica Minolta, Tokyo, Japan), a D65 light source and a 2° observer. The values were expressed as $L*$ (lightness), $a*$ (redness), and $b*$ (yellowness) units. A white standard plate was used to calibrate the colorimeter for the measurement of skin color. $L*$, $a*$, and $b*$ values were obtained at different locations of the smoked chicken thighs.

Image Preprocessing

In order to ensure that the color features can be extracted by the neural network model, a region of interest (**ROI**) with 384 × 384 pixels was extracted from each image. In this study, the DCGAN model (Chang and Scherer, 2017) was used to preprocess the images of smoked chicken thighs. The preprocessing methods in this study included random contrast adjustment, random brightness adjustment, random rotation, and random image scaling and adjustment (Chang and Scherer, 2017). The collected data could be divided into 2 major parts: a training set and a testing set. Here, 70% of the data set was randomly selected as a training set, and the rest of the data were used as a testing set.

Colorimetric Card Establishment

The color information at each resolution of the sample image was weighted to obtain the dominant color, and then a colorimetric card was produced based on the dominant color of the smoked chicken thighs at each time. Based on that, the 3 algorithms were used to obtain the dominant color of the sample image and produce the colorimetric card.

- *Colorimetric card constructed by the mean values algorithm.* As shown in Figure 2A, the original image was divided into several pixel blocks with a kernel size of 24 × 24, and the RGB value of each pixel block was obtained. With the kernel size of the pixel block gradually increased to 58 × 58→98 × 98→192 × 192, the local RGB value gradually transforms to the global RGB value. The dominant color of this image was obtained from the global RGB values. The dominant colors of the smoked chicken thighs for each smoking time were arranged sequentially by time, and the obtained dominant color sequence image was the colorimetric card produced by the mean value algorithm.
- *Colorimetric card produced by the K-means algorithm.* Figure 2B showed the main process of the K-means algorithm to produce colorimetric cards. A pixel block with 5 × 5 kernel size was extracted from the original image, and then a slider of size 2 × 2 with a step size of 1 was used to traverse the pixel block. After extracting the average RGB values of the pixel blocks in the red box, the slider will be moved one column to the right to obtain the average RGB values in the black box (Esfahani et al., 2016). All RGB information of pixel blocks was traversed and a total of 17 groups of RGB mean information of pixel blocks were extracted. There are 10 pixel block regions of kernel size 5 × 5 on each image of smoked chicken thighs. Then, the traversal results of all images were clustered by the K-means algorithm. The Euclidean distance between each point of a single class was calculated. Several initial cluster center points were

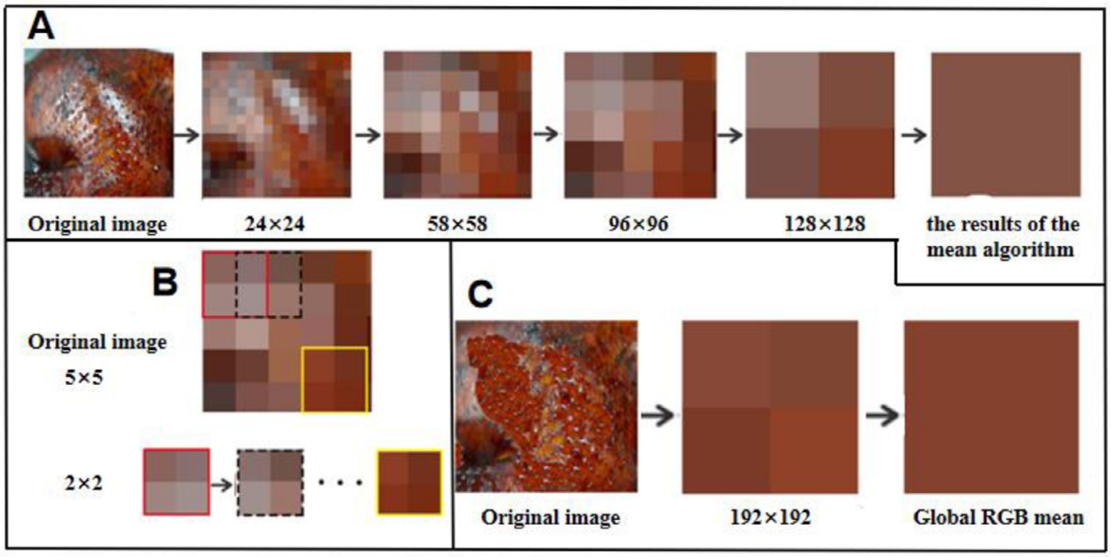

Figure 2. The process of constructing colorimetric cards with the three algorithms. (A) Mean value algorithm, (B) K-means algorithm, (C) K-means algorithm + image noise reduction algorithm.

determined. The RGB information of the central data in each category was extracted and averaged. Finally, the global RGB value of this image will be obtained.

- *Colorimetric card produced by the K-means algorithm + image noise reduction algorithm* (Zhang et al., 2019). Due to irregularities in the shape of the smoked chicken thighs and the thickness of the skin, the smoked chicken thighs samples may exhibit some variations in color, degrading the image quality. The poor quality of the image could be characterized by clustering the corrupted "dirty data" and "noise". Based on the K-means algorithm, the overall color deviation of the image will be reduced in this study by automatically replacing the color gamut of poor image quality with the surrounding areas. The method used an intelligent cleaning mode of "dirty data", which contributes to improving the accuracy of the colorimetric card. The 2 most important sources of "dirty data" were the reflections from photography and the darker areas of the smoked chicken thighs. The RGB value of the reflective areas tended to 0, while those of the dark parts tended to the maximum value. Through machine learning, the image was traversed to find areas where the RGB values were too low or too high. The center point of the K-means similar cluster was covered on the reflective surface and the area with a darker color and automatically replaced with normal color areas. Figure 2C showed that the reflections lead to a significant difference in the RGB values within the kernel size of 192 × 192 pixel blocks. The noise could be reduced by replacing the RGB values with the cluster center point value. Finally, the global RGB value of this image will be obtained.

Comparison of Colorimetric Card Accuracy

The colorimetric cards in this study were all produced based on the algorithm. The use of sensory analysis alone as a means of evaluation may be highly subjective and have large errors. There may be problems of poor generalization or data missing by using only algorithms as an evaluation means (Liu and Li, 2019). Therefore, this study used the K-medoids algorithm combined with sensory analysis to evaluate the accuracy of the 3 colorimetric cards.

- *Algorithm verifying the accuracy of colorimetric card recognition.* K-medoids algorithm (Hashemzadeh and Zademehdi, 2019), Use a slider of size 5 × 5 to divide each image into several regions, average the RGB colors of each region, and randomly select 17 points as the center point in the overall sample points (medoids). The selected medoids were randomly located in the current cluster (a total of 17 clusters) and the RGB values of the 17 clusters were compared with that of the 3 algorithms. The results were used as the main basis for evaluating the accuracy of the colorimetric card.
- *Sensory experiments verify the accuracy of colorimetric card recognition.* The training of sensory panelists was referred to the method of Liu et al. (2019). Eight panelists (2 female and 6 males, aged 20−26 yr) were selected as sensory panelists. The panelists were both students and staff of the School of Food Science and Engineering, Bohai University, who were physically healthy, colorblind, and able to distinguish color differences effectively (Carolina et al., 2014). Training of panelists was performed according to sensory evaluation procedure, and 8 panelists were trained with color identification for 2 wk for samples. The sensory evaluation focused on comparing the color of the samples with the colorimetric card to evaluate the smoking time of the actual samples. During the sensory evaluation, panelists were placed in private booths under the incandescent lights. The next sample was evaluated after about

3 min. A total of 14 sessions was performed, with 17 samples for each session.

The sensory experiment process was as follows: 1) Smoked chicken thighs with a smoking time of 0 to 16 min were used as samples and were labeled with 3-digit random numbers on the back of each sample and provided one at a time in random order. 2) The smoking time of the disordered samples was evaluated by the sensory panelists based on each of the 3 colorimetric cards. 3) The accuracy of 3 colorimetric cards for sensory analysis was obtained by comparing the smoke time obtained from sensory analysis with the correct smoke time.

The colorimetric card contains 17 different colors. Each color represents the corresponding time. For example, 0 indicates the color of the smoked chicken when it was not smoked, 16 indicates the color of the smoked chicken when the smoking time was 16 min. The experiment was repeated three times, and the final result was calculated as the mean of all sensory analyzes.

Statistical Analysis

The image processing algorithms, multiple regression algorithm, color information, and colorimetric card production were coded using Python programming language in OpenCV (Open-Source Computer Vision Library) platform and then uploaded to the device. All results were expressed as the means ± standard error. All graphs were draw up by using originPro 8.5 software (OriginLab Corporation, Northampton, MA). The goodness of fit of each model was evaluated using the coefficient of determination (R^2). All experiments were performed in at least 10 times.

RESULTS AND DISCUSSION

Image Acquisition and Preprocessing Results

There were 64 images of smoked chicken thighs for each smoking time, and a total of 1,088 images were collected for 17 smoking times. Based on these, 4 types of image preprocessing were used to obtain 256 images of smoked chicken thighs for each time, and a total of 4,352 images were obtained for 17 time periods. Defined as the dataset Smoked Chicken. The preprocessing results of the images were shown in Figure 3. Under the premise of not changing the properties of the image, random contrast and random brightness adjustment make the image present a difference in brightness, which was beneficial to obtain more image information. The original position, orientation, and magnitude of the images were changed after random rotation and random scaling. As a result, the new image generation not only increases the number of samples but also improves the accuracy of test results.

L*a*b* Values Results and Analysis

During the smoking process, the color of smoked chicken was mainly influenced by the smoking time, temperature, and materials. The study mainly controlled the color change of smoked chicken thighs by controlling the smoking time. The color changes of sugar-smoked chicken thighs for the different smoking

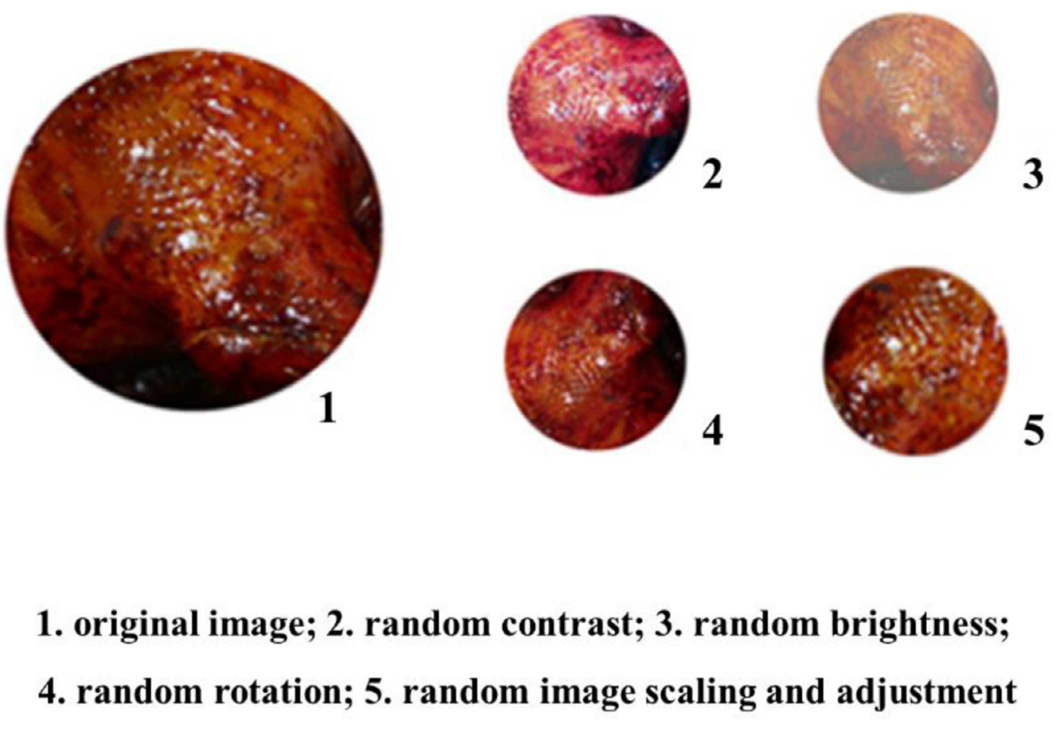

Figure 3. Image preprocessing results of smoked chicken thighs.

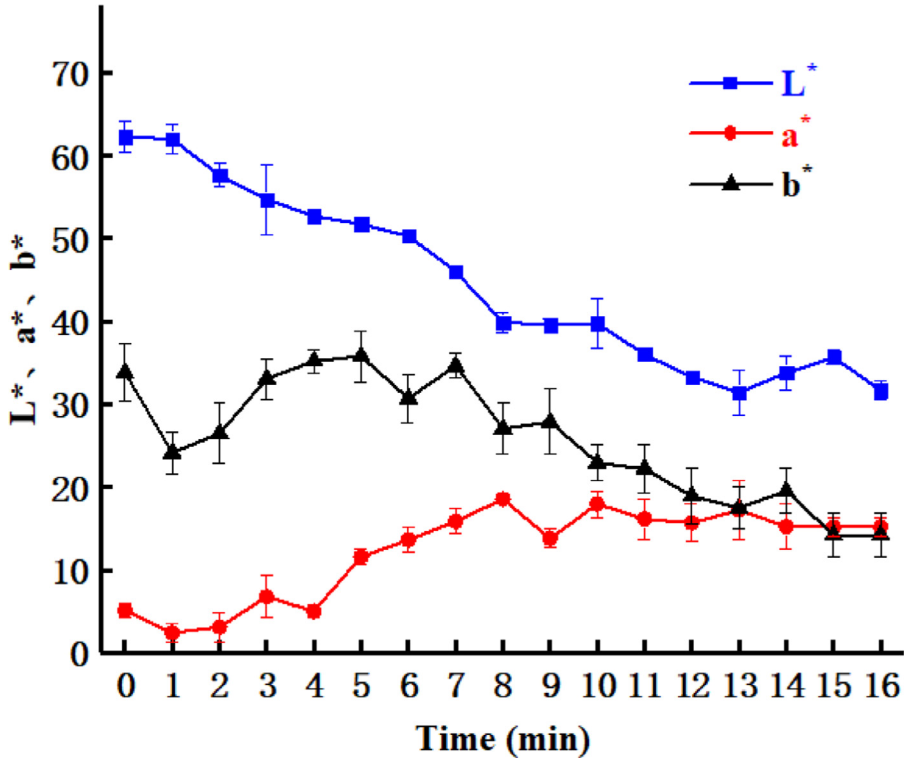

Figure 4. The variation of $L^*a^*b^*$ value of chicken thighs in smoked 0 to 16min. Bars represent standard deviation from triplicate determinations.

times were shown in Figure 4. The L^*, a^* and b^* values changed noticeably with the extension of the smoking time.

With the extension of smoking time, the L^* values of smoked chicken thighs generally showed a trend of decreasing (0–12 min) and then stabilizing (12–16 min). Similar results were reported by Morales and van Boekel (1998) and Zhang et al. (2021c), in which L^* values decreased significantly during the smoking process, indicating the increase of darkness. The research of Ledesma et al. (2015) demonstrated that the decrease of the L^* value was related to the decrease of water content in meat products during the smoking process and the deposition of a large number of soot particles on the surface of smoked foods. The a^* values increased at 1 to 9 min and have no differences at 9 to 16 min. According to Siskos et al. (2005), the a^* value was strongly correlated with the brown color intensity during the smoking process. The b^* value decreased significantly at 0 to 1 min, tended to increase significantly at 1 to 5 min, decreased significantly at 5 to 12 min, and had no difference at 12 to 16 min. The changes of a^* and b^* values may be the deposition of brown pigments from sugar smoking and reactions between smoke and food components, such as the Merald reaction, lipid oxidation (Siskos et al., 2005). At the smoking time of 0 to 1 min, the surface temperature of the chicken thighs was increased while the lipid oxidation reaction may have occurred to make the b^* decrease significantly. Subsequently, as the surface temperature of chicken thighs increased, the lipid oxidation products occurred with the chemical components of the smoke in a Merald reaction, causing the increase of the b^* value. There was no significant change in the values of L^*, a^*, and b^* when the smoking time was 12 to 16 min, which may be the result of oversmoking of smoked chicken thighs in this period and the samples were brown-black.

The $L^*a^*b^*$ values fluctuated from 1.70 to 3.59 for L^*, 0.61 to 2.17 for a^*, and 0.89 to 4.21 for b^* at each smoking time. The main reason for this situation was the change in furnace temperature. Although the furnace temperature was reached at the beginning of the study, the box temperature inevitably fluctuated with the opening operation when the sample was put in and the sucrose was added. The color variations of smoked chicken thighs were all within a reasonable range. There was no significant difference in the color of the samples under the same smoking time, and the color of the samples under different smoking times showed a significant gradient change, indicated that the process matured with good stability.

Colorimetric Card Establishment Results

The production results of the 3 colorimetric cards were shown in Figure 5. Compared with Figures 5A and 5B, the colorimetric card of Figure 5C has a richer color variation. This is due to the algorithm differences. These color changes can be easily distinguished by the naked eye. Sucrose was formed as a monosaccharide by breaking the glycosidic bond after pyrolysis at 330°C. The monosaccharide was dehydrated and decarbonized after isomerization reaction and produce smaller molecular weight furfural, 5-hydroxymethyl furfural and other pyrolysis products (Carolina and Varoujan, 2008;

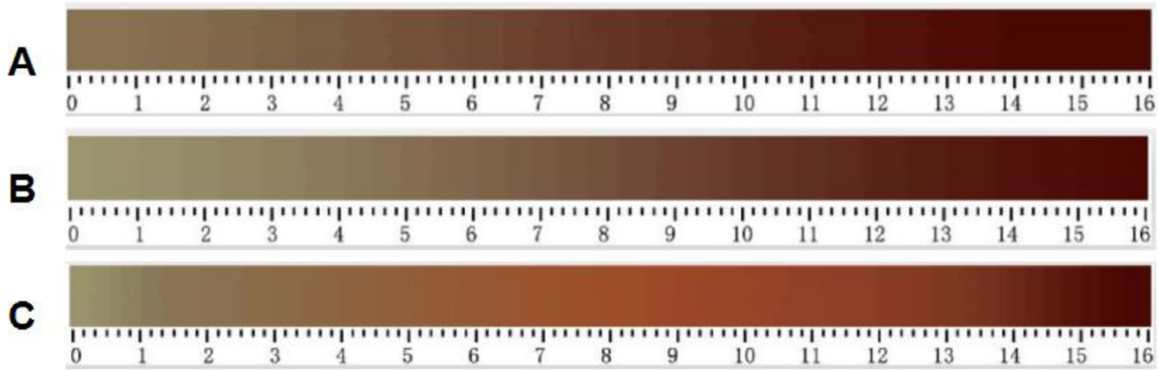

Figure 5. Colorimetric cards produced by the three algorithms. (A) →Mean value algorithm, (B) →K-means algorithm, (C) →K-means algorithm + image noise reduction).

Ledesma et al., 2015; Sikorski, 2016). The sucrose pyrolysis products, such as furfural, penetrated the samples together with the fumes and occurred the Millard reaction and caramelization reaction with lipid oxidation products of chicken thighs at the temperature of 100°C. It was demonstrated that the brown pigment from sugar-smoked chicken has a similar structure to the melanin produced by the Maillard reaction (Echavarría et al., 2012). The brown pigment was composed of various chemotactic components, which mainly included polymers of fructose and glucose and derivatives from lipid oxidation. This may be the primary reason for the brown skin of the sugar-smoked chicken thighs.

It can be observed that the color of the colorimetric card became darker with the increase in smoking time (Figure 5). As demonstrated by Angel et al. (2004) that the smaller the molecular weight of the compound, the stronger the Maillard reaction activity. Some studies indicated that with the increase of temperature and time, more denatured proteins would be involved in the Maillard reaction, which leads to an increase in the intensity of glycosylation and browning, accumulation of melanin, and deepening the surface color (Lee et al., 2017).

From the R value information of the 3 colorimetric cards in Figure 6A, the R value of the K-means

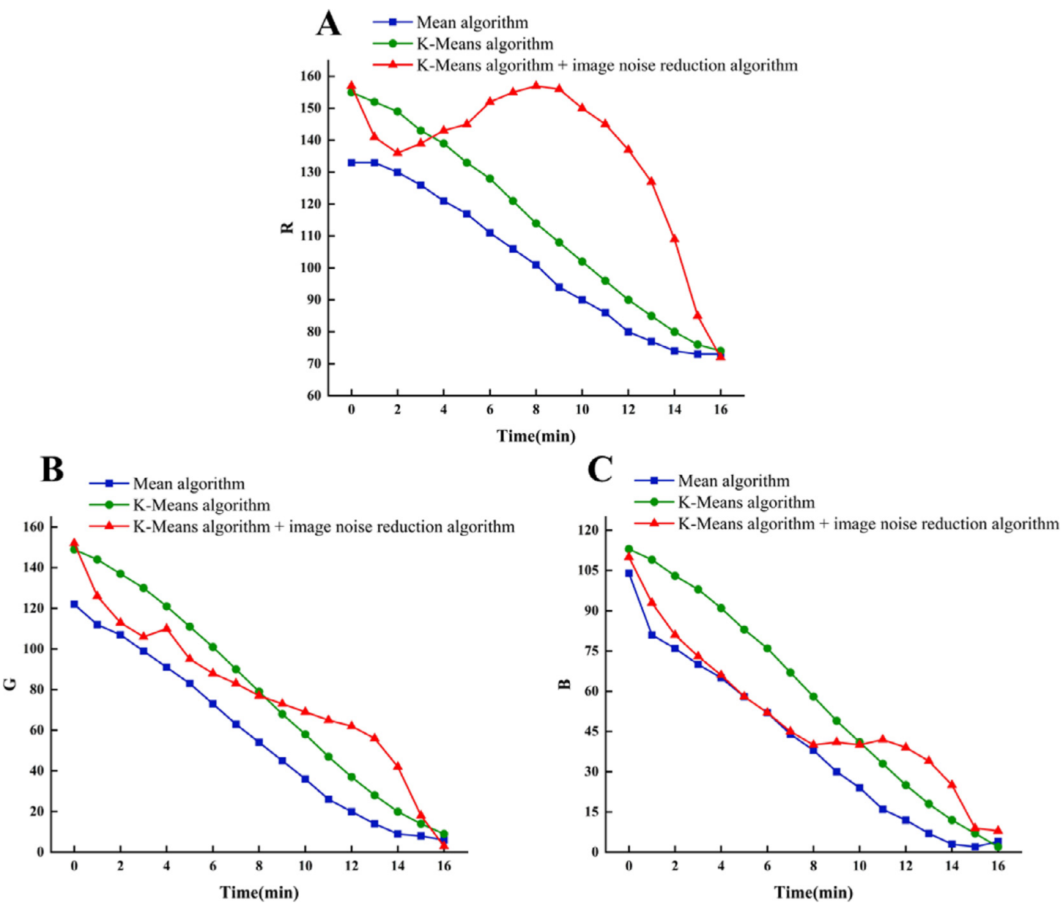

Figure 6. RGB value information of the three colorimetric cards. (A) → R value of the three colorimetric cards, (B) → G value of the three colorimetric cards, (C) → B value of the three colorimetric cards).

Table 1. Multiple regression model of RGB value information and smoking times of 3 colorimetric cards.

Algorithm	Model	(R^2)[1]
Mean value	Y = 18.765-0.052R-0.101G+0.006B	0.986
K-means	Y = 13.685+0.038R-0.127G-1.442B	0.995
K-means + noise reduction	Y = 13.779+0.5R-0.204G+0.7B	0.952

[1]R^2: The determining coefficient, reflecting the proportion of all variations in the dependent variable that can be explained by the independent variable through regression relations.

algorithm + image noise reduction processing algorithm was higher than that of the K-means algorithm and means algorithm. The color change in the colorimetric card showed a more uniform trend of decreasing red gradient after 6 min, probably due to the image noise reduction process which removed a large number of extreme values (Zhang et al., 2019). As seen in Figures 6B and 6C, there was no evident difference between the G and B values of the 3 colorimetric cards.

In addition, the multiple linear regression analysis was performed between the RGB values of the 3 colorimetric cards and the corresponding smoked time. As shown in Table 1, the correlation coefficients (R^2) of the mean algorithm, K-mean algorithm and K-mean algorithm + image noise reduction algorithm were 0.986, 0.995, and 0.952, respectively. The correlation coefficients of the 3 algorithms all exceeded 0.950, indicated that the equations fit well and can reflect the relationship between the smoking time and the corresponding color information. It indicated that the colorimetric card can identify and classify the smoked stages of smoked chicken thighs.

Colorimetric Card Recognition Accuracy Results

The accuracy of the 3 colorimetric cards was 87.2% for the Mean algorithm, 95.1% for the K-means algorithm, and 96.7% for the K-means algorithm + image noise reduction processing algorithm from Figure 7. The accuracy of the sensory analysis of the mean algorithm, K-means algorithm, and K-means algorithm + image noise reduction algorithm for colorimetric cards was 54.9, 67.2, and 63.9%, respectively. The negative sensory identification results were due to oversmoking of all samples smoked for 12 to 16 min, with darker colors and no significant color differences. Thus, the accuracy was recalculated in this study by removing the sensory data from 12 to 16 min. It showed that the sensory recognition accuracy of colorimetric cards for the mean algorithm, K-means algorithm, and K-means algorithm + image noise reduction processing algorithm was 69.4, 80.9, and 79.2%, respectively (Figure 7).

The accuracy sequence of sensory verification (K-means algorithm > K-means algorithm + image noise reduction > Mean values algorithm) and that of algorithm verification (K-means algorithm + image

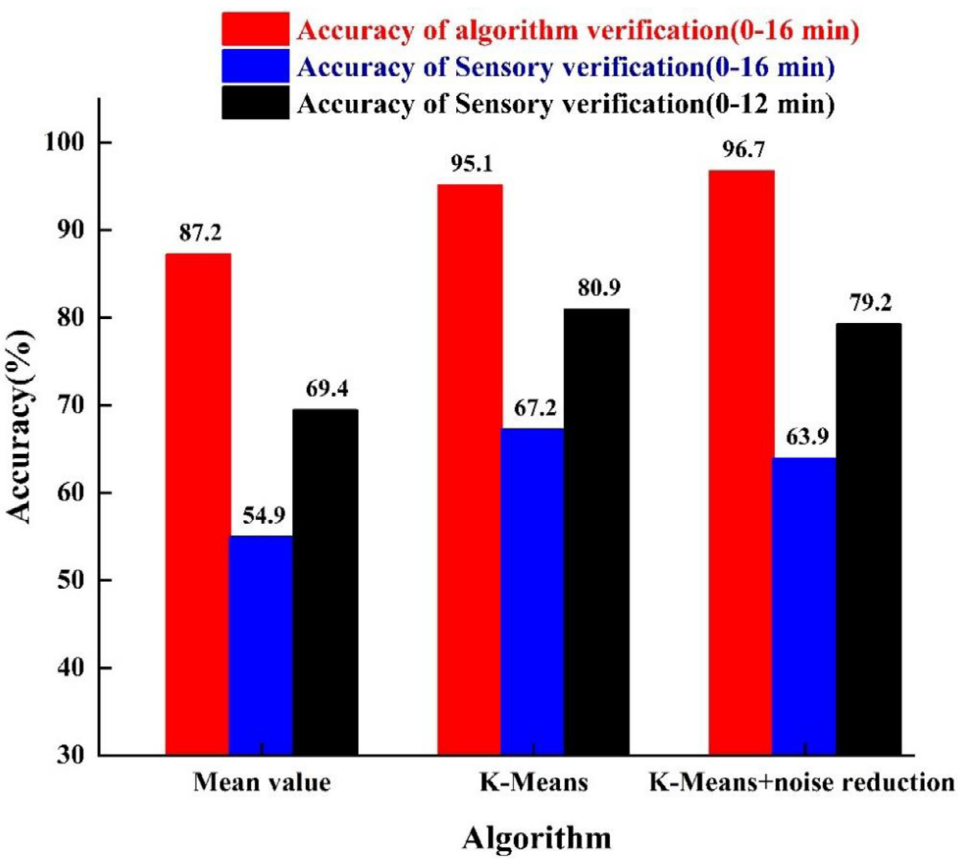

Figure 7. The sensory recognition accuracy (0−16 min and 0−11 min) and algorithm recognition accuracy (0−16 min) of the three colorimetric cards.

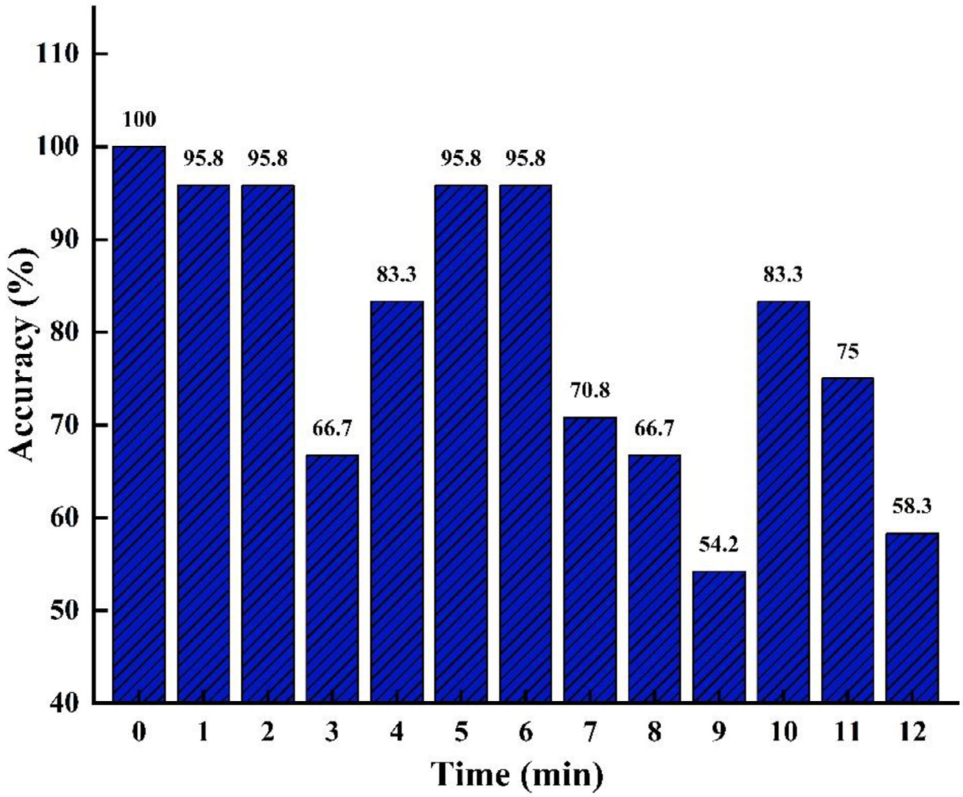

Figure 8. The accuracy of the sensory analysis of the colorimetric cards produced by the K-means algorithm at each time.

degradation noise processing > K-means algorithm > mean values algorithm) do not match. The reason may be that the K-means algorithm + image noise reduction removes a large amount of abnormal and extreme data (reflective areas and dark areas) when processing the image data (Zhang et al., 2019). Therefore, the K-means algorithm + image noise reduction processing algorithm of the colorimetric card had the highest accuracy in algorithm verification results, and the K-means algorithm had the highest accuracy of the colorimetric card in sensory evaluation results. The accuracy of the sensory analysis of the colorimetric cards produced by the K-means algorithm at each time was shown in Figure 8. The accuracy of smoking time at 0, 1, 2, 5, 6, and 10 min was 100, 95.8, 95.8, 83.3, 95.8, and 83.3%, respectively. The accuracy was 66.7, 66.7, 70.8, 66.7, and 54.2% for smoking times of 3, 4, 7, 8, and 9 min, respectively. The low accuracy of the smoking time at the 3 and 4 min may be due to the color of the surface of the smoked chicken thighs only gradually deepened from light yellow to brownish-yellow with the increase of the smoking time color difference was not significant. The accuracy of sensory recognition was low for the smoking times at 7, 8, and 9 min, probably attributed to the color change in a relatively stable process after the more significant period (6 min, as shown in Figure 4). There was no significant color change on the surface of smoked chicken thighs at the smoking time between 7, 8, and 9 min, which led to low accuracy of sensory analysis. In addition, according to the colorimetric card produced by the K-means algorithm, we concluded that the smoked color was better at 7, 8, and 9 min, and the best-smoked color was generated at 8 min.

CONCLUSIONS

In this article, we applied machine vision technology to quickly identify the color of sugar-smoked chicken thighs and establish the corresponding colorimetric cards using the mean value algorithm, K-means algorithm, and K-means algorithm + image noise reduction processing algorithm. Sensory analysis and K-medoids algorithms were utilized to verify the accuracy of the colorimetric cards. The production results of colorimetric cards showed that all 3 colorimetric cards had a good gradient change of color. The algorithmic recognition accuracy of the 3 colorimetric cards was 87.2% for the Mean algorithm, 96.7% for the K-Means algorithm, and 95.1% for the K-means algorithm + image noise reduction processing algorithm, and the sensory recognition accuracy was 69.4% for the mean algorithm, 80.9% for the K-means algorithm, and 79.2% for the K-means algorithm + image noise reduction processing algorithm. Overall, the colorimetric cards produced by K-means algorithm and K-means algorithm + image noise reduction algorithm had an excellent accuracy and good sensory attributes, which can achieve fast and accurate color identification of smoked chicken. Meanwhile, the colorimetric card can guide consumers to purchase smoked chicken products, for enterprises to monitor their production and processing processes, and for other products related to color identification research.

ACKNOWLEDGMENTS

This work was supported by "National Key R&D Program of China (No. 2016YFD0401505)" and "LiaoNing Revitalization Talents Program (XLYC1807100)". The authors thank AiMi Academic Services (www.aimieditor.com) for English language editing and review services.

DISCLOSURES

The authors have declared no conflict of interest.

REFERENCES

Alakali, J. S., O. O. Adekoyeni, I. C. Alaka, J. Faasema, and T. Torvor. 2017. Fabrication and performance evaluation of a hybrid fish smoking kiln. Food Process. Preserv. 41:e12935.

Angel, R. H. J., G. V. Belén, and G. H. Eduardo. 2004. Generation of furosine and color in infant/enteral formula-resembling systems. J. Agric. Food Chem. 52:5354–5358.

Bahr, K. D., S. J. L. Severino, A. O. Tsang, J. J. Han, A. Richards Dona, Y. O. Stender, R. M. Weible, A. Graham, A. E. McGowan, and K. S. Rodgers. 2020. The Hawaiian Ko'a Card: coral health and bleaching assessment color reference card for Hawaiian corals. SN Appl. Sci. 2:837–850.

Brosnan, T., and D. W. Sun. 2004. Improving quality inspection of food products by computer vision—a review. J. Food Eng. 61:3–16.

Carolina, M. G., R. B. J. José, M. A. M. Victoria, and P. B. M. Ángeles. 2014. Feasibility and application of a retronasal aroma-trapping device to study in vivo aroma release during the consumption of model wine-derived beverages. Food Sci. Nutr. 2:361–370.

Carolina, P. L., and A. Y. Varoujan. 2008. Isotope labeling studies on the formation of 5-(hydroxymethyl)-2-furaldehyde (HMF) from sucrose by pyrolysis-GC/MS. J. Agric. Food Chem. 56:6717–6723.

Chang, J., and S. Scherer. 2017. Learning representations of emotional speech with deep convolutional generative adversarial networks. Proc. ICASSP 2017 - 2017 IEEE International Conference on Acoustics, Speech and Signal Processing (ICASSP). IEEE, New Orleans, LA.

Chang, H., Y. Wang, Q. Xia, D. Pan, J. He, H. Zhang, and J. Cao. 2021a. Characterization of the physicochemical changes and volatile compound fingerprinting during the chicken sugar-smoking process. Poult. Sci. 100:377–387.

Chang, H., C. Y. Zhou, J. He, D. D. Pan, Y. Wang, X. Zhang, and J. X. Cao. 2021b. Identifying and characterizing the components related to the brown color of Chinese sugar-smoked chicken during processing. Poult. Sci. 100:100937.

Echavarría, A. P., J. Pagán, and A. Ibarz. 2012. Melanoidins formed by maillard reaction in food and their biological activity. Food Eng. Rev. 4:203–223.

Esfahani, R. K., F. Shahbazi, and M. Akbarzadeh. 2016. Three phase classification of an uninterrupted traffic flow: a k-means clustering study. Transp. Metr. B. 7:546–558.

Gary R, Z. D., M. D. R. Trellis, M. T. Sherman, and M. R. Clouse. 1995. An objective measure of stool color for differentiating upper from lower gastrointestinal bleeding. Dig. Dis. Sci. 40:1614–1621.

Giuseppe, V., S. Jörn, S. Frauke, F. Matthias, K. Oliver, and A. H. Marianne. 2008. Evaluation of new colorimetric vitek 2 yeast identification card by use of different source media. J. Clin. Microbiol. 46:3784–3787.

Hashemzadeh, M., and A. Zademehdi. 2019. Fire detection for video surveillance applications using ICA K-medoids-based color model and efficient spatio-temporal visual features. Expert Syst. Appl. 130:60–78.

Janky, D. M., J. L. Oblinger, and J. A. Koburger. 1975. Sensory and microbiological evaluation of smoked cornish game hens. Poult. Sci. 54:1942–1945.

Ledesma, E., M. Rendueles, and M. Díaz. 2015. Characterization of natural and synthetic casings and mechanism of BaP penetration in smoked meat products. Food Control. 51:195–205.

Lee, Y. Y., T. K. Tang, E. T. Phuah, N. B. M. Alitheen, C. P. Tan, and O. M. Lai. 2017. New functionalities of Maillard reaction products as emulsifiers and encapsulating agents, and the processing parameters: a brief review. J. Sci. Food. Agric. 97:1379–1385.

Liu, D., and J. Li. 2019. Safety monitoring data classification method based on wireless rough network of neighborhood rough sets. Saf. Sci. 118:103–108.

Liu, H., Z. Wang, R. Suleman, Q. Shen, and D. Zhang. 2019. Effect of protein thermal stability and protein secondary structure on the roasted mutton texture and colour from different cuts. Meat Sci. 156:52–58.

Misimi, E., J. R. Mathiassen, and U. Erikson. 2007. Computer vision-based sorting of Atlantic salmon (Salmo salar) fillets according to their color level. J. Food Sci. 72:030–035.

Morales, F. J., and M. A. J. S. van Boekel. 1998. A study on advanced Maillard reaction in heated casein/sugar solutions: colour formation. Int. Dairy J. 8:907–915.

Paravisini, L., A. Prot, C. Gouttefangeas, C. Moretton, H. Nigay, C. Dacremont, and E. Guichard. 2015. Characterisation of the volatile fraction of aromatic caramel using heart-cutting multidimensional gas chromatography. Food Chem. 167:281–289.

Purlis, E. 2012. Baking process design based on modelling and simulation: towards optimization of bread baking. Food Control. 27:45–52.

Purlis, E., and V. O. Salvadori. 2009. Modelling the browning of bread during baking. Food Res. Int. 42:865–870.

Reyescerecedo, A., J. Florescalderón, M. Villasiskeever, J. Chávezbarrera, and E. Delgadogonzález. 2018. Colorimetric card use for early detection visual biliary atresia. Bol Med. Hosp Infant. Mex. 75:160–165.

Roberta, A., L. Daniela, P. Monica, P. Andrea, M. S B., M. Antonella, S. Samira, G. Chiara, M. C S., C. Manila, M. Giuseppe, and S. Marco. 2020. A novel mobile phone application for infant stool color recognition: an easy and effective tool to identify acholic stools in newborns. J. Med Screen. 27:184–189.

Schwert, R., R. Verlindo, A. J. Cichoski, D. Oliveira, and E. Valduga. 2011. Comparative evaluation of liquid and traditional smoke on oxidative stability, color and sensory properties of Brazilian calabrese sausage evaluación comparativa del ahumado tradicional y líquido en la estabilidad oxidativa, propiedades de color y sensoriales de la salchicha calabresa brasileña. CYTA J. Food. 9:131–134.

Sheldon, B. W., H. R. Ball, and H. R. Kimsey. 1982. A comparison of curing practices and sodium nitrite levels on the chemical and sensory properties of smoked turkey. Poult. Sci. 61:710–715.

Shi, C., J. Qian, S. Han, B. Fan, X. Yang, and X. Wu. 2018. Developing a machine vision system for simultaneous prediction of freshness indicators based on tilapia (Oreochromis niloticus) pupil and gill color during storage at 4 degrees C. Food Chem. 243:134–140.

Sikorski, Z. E. 2016. Smoked foods: principles and production. Encycl. Food. Health. 18:1–5.

Siskos, I., A. Zotos, and K. D. A. Taylor. 2005. The effect of drying, pressure and processing time on the quality of liquid-smoked trout (Salmo gairdnerii) fillets. J. Sci. Food. Agric. 85:2054–2060.

Taheri-Garavand, A., S. Fatahi, M. Omid, and Y. Makino. 2019. Meat quality evaluation based on computer vision technique: a review. Meat Sci. 156:183–195.

Valous, N. A., M. Fernando, D. W. Sun, and P. Allen. 2009. Colour calibration of a laboratory computer vision system for quality evaluation of pre-sliced hams. Meat Sci. 81:132–141.

Vladimir, S., D. Olha, K. Halyna, H. Taras, and G. Mykhailo. 2011. Alcohol oxidase and formaldehyde dehydrogenase-based enzymatic methods for formaldehyde assay in fish food products. Food Chem. 127:774–779.

Wang, H. H., and D. W. Sun. 2003. Assessment of cheese browning affected by baking conditions using computer vision. J. Food Eng. 56:339–345.

Zhang, L., H. Du, P. Zhang, B. Kong, and Q. Liu. 2020. Heterocyclic aromatic amine concentrations and quality characteristics of traditional smoked and roasted poultry products on the northern Chinese market. Food Chem. Toxicol. 135:e110931.

Zhang, L., Y. Hu, Y. Wang, B. Kong, and Q. Chen. 2021a. Evaluation of the flavour properties of cooked chicken drumsticks as affected by sugar smoking times using an electronic nose, electronic tongue, and HS-SPME/GC-MS. Lwt 140:110764.

Zhang, N., Q. Hu, L. Wang, S. Meng, R. Pan, and W. D. Gao. 2021b. Appearance change for colored spun yarn fabric based on image color transfer. Text Res J. 91:1439–1451.

Zhang, D., K. Shi, Z. Guo, and B. Wu. 2019. A class of elliptic systems with discontinuous variable exponents and L 1 data for image denoising. Nonlinear. Anal. Real World Appl. 50:448–468.

Zhang, L., H. Wang, X. Xia, M. Xu, B. Kong, and Q. Liu. 2021c. Comparative study on the formation of heterocyclic aromatic amines in different sugar smoking time. Food Control. 124:107905.